nature physics

ARTICLES

PUBLISHED ONLINE: 21 MARCH 2010 | DOI: 10.1038/NPHYS1621

Interplay between superconductivity and ferromagnetism in crystalline nanowires

Jian Wang[1,2]*, Meenakshi Singh[1,2], Mingliang Tian[1,2], Nitesh Kumar[1,2†], Bangzhi Liu[3], Chuntai Shi[1,2†], J. K. Jain[1,2], Nitin Samarth[1,2], T. E. Mallouk[1,2,4] and M. H. W. Chan[1,2]*

The interaction between superconductivity and ferromagnetism, which entails incompatible spin order, is one of the problems of fundamental interest in condensed-matter physics. In general, when a ferromagnet is placed in contact with a superconductor, the Cooper pairs from the superconductor are not expected to survive beyond at most a few nanometres into the ferromagnet. Here we present a systematic study of single-crystal ferromagnetic cobalt nanowires sandwiched between superconducting electrodes. Surprisingly, we find that a cobalt wire as long as 600 nm attains zero resistance at low temperatures. For even longer nanowires, the transition to incomplete superconductivity is foreshadowed by a strikingly large and sharp resistance peak near the superconducting transition temperature of the electrodes. Although the origin of the 'critical peak' remains mysterious, our analysis strongly points against charge or spin imbalance as its underlying cause.

Near a superconductor/normal-metal interface, the leakage of Cooper pairs extends superconducting behaviour into the metal. This is known as the proximity effect, the spatial range of which can be as long as ∼1 μm (refs 1,2). Despite a long history of the study of the proximity effect in various geometries and materials, new insights continue to emerge from measurements in new systems such as nanowires. For instance, in a recent four-probe transport measurement of single-crystal gold nanowires, we found a systematic evolution of the proximity effect with increasing separation between superconducting tungsten (W) electrodes[3]. However, when a ferromagnet is in contact with an *s*-wave superconductor, superconductivity is expected to decay rapidly (a few nanometres) inside the ferromagnet owing to the incompatible nature of superconductivity and ferromagnetic order[4]. This expectation was confirmed in macroscopic (Fe, Ni)–In junctions[5] and submicrometre Ni–Al structures[6] where the spatial range of the proximity effect is limited to ∼1 nm. On the other hand, a surprisingly long-ranged proximity effect was found in a number of experiments on mesoscopic superconductor–ferromagnet hybrid structures[7–12]. In particular, a recent experiment detected supercurrent in a half-metallic ferromagnet CrO_2 thin film sandwiched between two singlet superconducting electrodes separated by 1 μm (ref. 12). To account for the unusually long-ranged proximity effect, the induced superconductivity in the CrO_2 film was attributed to spin-triplet pairing instead of the usual singlet state[7,13].

Here, we report the observation of a long-ranged proximity effect in an ordinary hard ferromagnetic crystalline nanowire. We have studied four Co nanowires in the standard four-probe configuration with different separations between the voltage electrodes. Measurements are carried out on samples with all four electrodes made from superconducting W, as well as samples with a combination of superconducting W and non-superconducting Pt electrodes. We have also made measurements where a superconducting W strip is placed in contact with the Co nanowire, but is not part of the measurement circuit: the proximity effect persists in this configuration. Our key findings are that Co nanowires are driven completely superconducting with zero resistance when sandwiched between two superconducting electrodes separated by 600 nm; that longer nanowires with 1.5 μm electrode separation show a substantial resistance drop but the resistance remains non-zero in the low-temperature limit; and that in these longer nanowires, the resistance shows a large and sharp 'critical peak' near the superconducting transition temperature of the W electrode.

The Co nanowires used in our experiments are fabricated by direct electrodeposition into the nanochannels of an anodized aluminium oxide (AAO) membrane[14]. High-resolution transmission electron microscopy (TEM) analysis showed that both the 40-nm- (Fig. 1a) and the 80-nm-diameter Co nanowires are single crystal with hexagonal close-packed structure. We note that the fabricated nanowires have a variation of ±5 nm in diameter because of the variation in the pore size of the AAO membrane. The oxide shell of 2 nm in thickness (Fig. 1a) protects the nanowires from contamination during the attachment of the electrodes. Magnetic force microscopy measurements at room temperature clearly indicate that the nanowires are ferromagnetic. To make ohmic electrical contact to individual Co nanowires, we dispersed the nanowires on a silicon substrate with a 1-μm-thick Si_3N_4 insulating layer. The sample was then transferred into a focused ion beam (FIB) etching and deposition system for the deposition of electrodes[15–17]. Four FIB-assisted superconducting W electrodes were deposited to contact an individual Co nanowire for a standard four-probe measurement (see Fig. 1b, inset). In the process of W electrode preparation, Ga^+ imaging was suspended to minimize gallium contamination of the nanowire. During the deposition, the chamber pressure was lower than 10^{-5} torr and the deposition FIB current was set below 20 pA to reduce the spread of the W electrodes. The FIB-deposited amorphous W strips are superconducting with T_C between 4.4 and 5.1 K depending on the exact deposition parameters of the FIB process (Supplementary Fig. S1); this is much

[1]The Center for Nanoscale Science; [2]Department of Physics; [3]Materials Research Institute; [4]Department of Chemistry, The Pennsylvania State University, University Park, Pennsylvania 16802-6300, USA. †Present addresses: Intel Corporation, 2501 NW 229th Avenue, Hillsboro, Oregon 97124, USA (N.K.); Department of Physics and Astronomy, University of California, Riverside, California 92521, USA (C.S.). *e-mail: juw17@psu.edu; chan@phys.psu.edu.

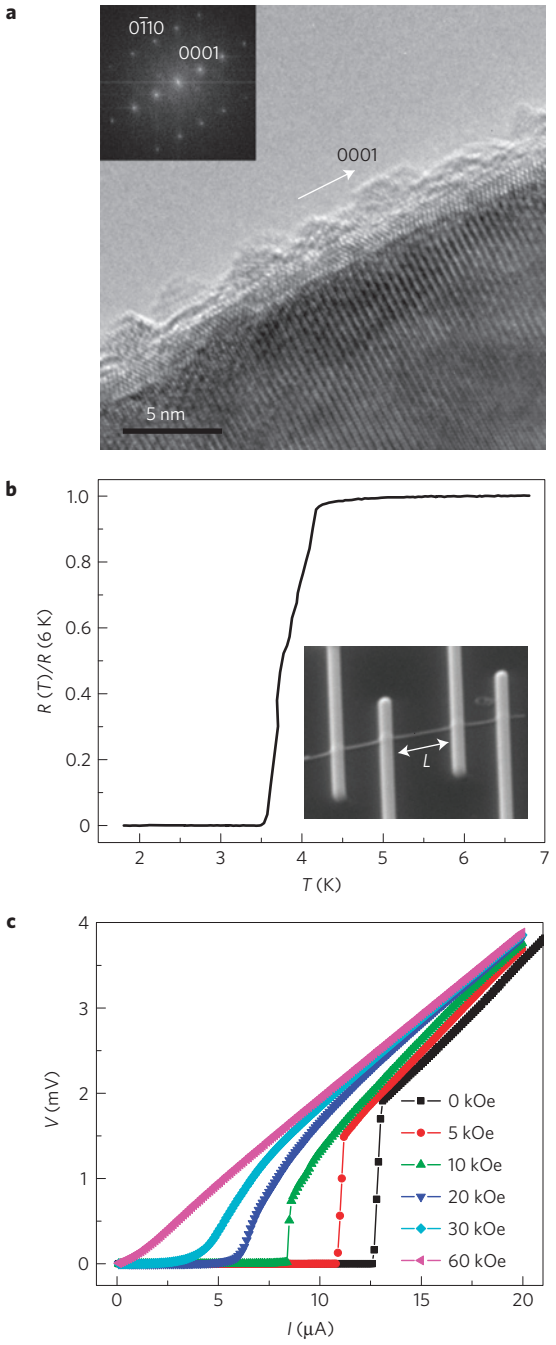

Figure 1 | TEM characterization and transport measurement of a 40 nm Co nanowire, with $L = 0.6$ μm. a, An oxide shell is found surrounding the crystalline core. The fast Fourier transform of the core (inset) shows a hexagonal close-packed [2 $\bar{1}$ $\bar{1}$ 3] zone pattern and [0001] growth direction. **b**, Zero resistance is found below 3.5 K. The inset is a scanning electron micrograph of the Co nanowire contacted by four FIB-deposited superconducting W electrodes. **c**, Voltage versus current curves of the Co nanowire measured at different perpendicular magnetic fields at 1.8 K. The lengths of the nanowires (L) in this article are defined to be the distance between the inner edges of the voltage electrodes. The resistance at 6 K is 193 Ω and the resistivity (ρ) of the wire, assuming an oxide shell of 2 nm, is 32 μΩ cm.

higher than the T_C of pure W (~12 mK) because the FIB-deposited W strips actually contain approximately 40% atomic carbon and 20% atomic gallium[18,19]. The W strips fabricated in this study are typically 250 nm wide and 100 nm thick and the contact resistance of the W–Co junction (Supplementary Fig. S2) is ~1 Ω. A small contact resistance is achieved by etching away the oxidation layer of the nanowires during the FIB deposition process. In a control experiment, the resistance between two parallel W strips separated by less than 500 nm on a Si_3N_4 substrate was measured to be larger than 10^5 Ω at 1.8 K, indicating an absence of direct leakage between the W strips (Supplementary Fig. S3). In another control experiment, TEM showed that the diffusion of the W atoms along Co wires is limited to within 200 nm from the edge of the W strips (Supplementary Fig. S4). It should be noted that the gallium ions used in the FIB patterning process are not responsible for the observed superconductivity because the FIB-deposited Pt strips also contain gallium but are not superconducting[15,16].

Figure 1b shows resistance as a function of temperature (R–T) for an individual 40 nm Co nanowire with a length of $L = 600$ nm. The vertical scale is normalized to the resistance at $T = 6$ K and the excitation current is 50 nA. The Co nanowire shows an onset of superconductivity near 4.2 K, slightly lower than that of the W electrode strip. Zero resistance, defined as a resistance smaller than the instrumental resolution (0.2 Ω for 50 nA excitation current), is found below $T = 3.5$ K. Measurements with an excitation current of 1 μA also show zero resistance below $T = 3.5$ K with a resolution of 0.01 Ω. This result indicates that the spatial extent of the proximity-effect-induced superconductivity in the Co nanowire is at least 300 nm.

The proximity-induced superconductivity in Co nanowires shows strong anisotropy under the application of a magnetic field. The magnitude of the perpendicular critical field at 1.8 K is approximately one-half that of the parallel critical field, consistent with expectations for a thin superconducting nanowire[20]. The voltage–current (V–I) characteristics at different perpendicular fields (Fig. 1c) show standard critical current behaviour. The critical current (I_C) at zero field at 1.8 K is comparable to that observed in single-crystal 40-nm-diameter superconducting Sn nanowires[21].

Figure 2 shows resistance as a function of temperature for two Co nanowires of the same length ($L = 1.5$ μm) but different diameters (40 and 80 nm) at different magnetic fields. (In this article, unless noted otherwise, the magnetic field is applied perpendicular to the wire axis.) Although the wires are not fully superconducting at 1.8 K, the lowest temperature of the experiment, the residual resistance of the 40 nm (80 nm) wire is 11% (50%) of the normal-state value. This suggests that the spatial extent of the proximity effect for the 40 nm wire is of the order of 500 nm, and also that the proximity effect extends to longer lengths in the thinner wire.

The most striking and unexpected result is the very large resistance peak (25% of the normal-state resistance for the 40 nm wire and ~100% for the 80 nm wire) found between 5 K and 4.5 K, just above the temperature of the superconducting resistance drop. With increasing field, the magnitude of the critical peak is suppressed as it moves to lower temperatures. The critical peak in the 40 nm nanowire is preceded by a small dip on the high-temperature side of the peak. Measurements in both warming up and cooling down scans show an absence of hysteretic behaviour. Both the peak and the superconducting drop are stable on cycling the sample to room temperature. Comparison with the proximity effect study of 70-nm-diameter single-crystal Au nanowires with W electrode separation of 1, 1.2 and 1.9 μm, where the spatial extent of the proximity effect was found to be between 600 and 950 nm (ref. 3), leads us to a surprising conclusion: the spatial extent of the proximity effect seems to be insensitive to whether the nanowire is a ferromagnetic or a standard paramagnetic metal. However, the critical peak was not seen in any of the Au wires and seems to be a consequence of the ferromagnetism of the Co wires.

Resistance (R) as a function of the magnetic field (H) at different temperatures for the 80 nm nanowire is shown in Fig. 3a. At 3 K,

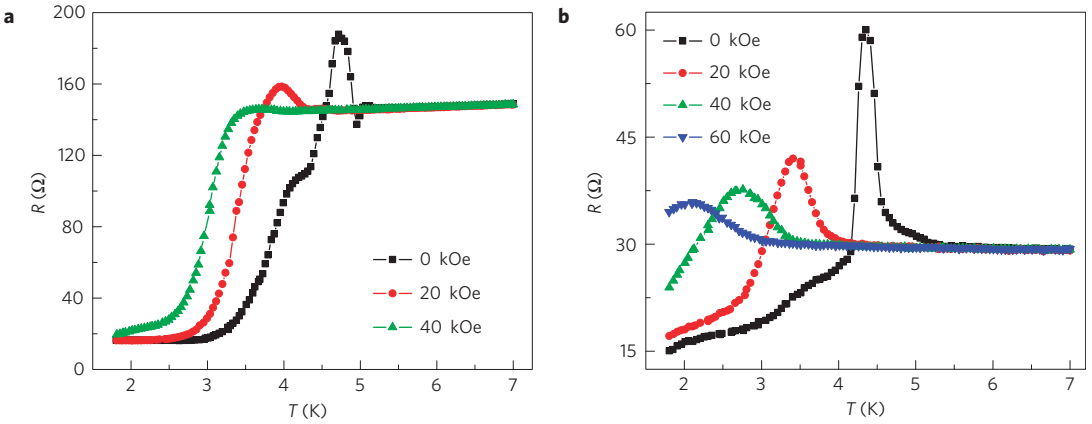

Figure 2 | *R–T* behaviour of 1.5-μm-long Co nanowires contacted by superconducting electrodes. a, Resistance as a function of temperature at different fields for an individual 40 nm Co nanowire with $L = 1.5\,\mu m$. ρ at 6 K is 10 μΩ cm. **b**, Resistance as a function of temperature at different perpendicular magnetic fields for an individual 80 nm Co nanowire with the same length ($L = 1.5\,\mu m$). ρ at 6 K is 9 μΩ cm.

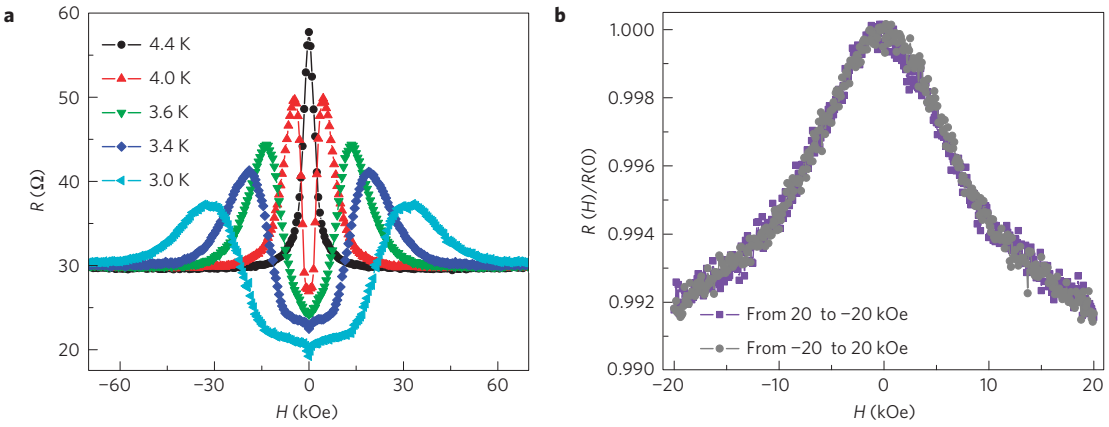

Figure 3 | *R–H* property and AMR effect of the 80 nm Co nanowire. a, Resistance versus magnetic field of the 80 nm Co nanowire, with $L = 1.5\,\mu m$, measured at the temperatures 4.4, 4.0, 3.6, 3.4 and 3.0 K. **b**, Magnetoresistance behaviour of the 80 nm Co nanowire, with $L = 1.5\,\mu m$, at 5.8 K.

the magnetoresistance peaks are symmetric under the change in the direction of the magnetic field. With increasing temperature, the two peaks move towards zero field and merge into a single peak at 4.4 K. Furthermore, the 3-K and the 3.4-K isotherms show a narrow dip in R at zero field in addition to the usual R versus H valley. This extra narrow dip is similar to that found in the 1.2- and 1.9-μm-long Au nanowires showing incomplete proximity-induced superconductivity[3]. No hysteresis was observed. Figure 3b shows the anisotropic magnetoresistance (AMR) effect of a Co nanowire above T_C, confirming the ferromagnetic property of the Co nanowire[22,23]. This AMR effect is also found when the ferromagnetic nanowires are contacted with normal Pt electrodes (see Supplementary Fig. S5).

To explore the precise role of the superconducting electrodes, we carried out the following control experiment. A 40 nm Co nanowire was contacted with two W strips as current electrodes and two normal Pt strips as voltage electrodes. The scanning electron micrograph (Fig. 4a, inset) shows that the lengths of the Co wire between the neighbouring inner edges of the W–Pt–Pt–W strips are respectively 0.8, 2.4 and 1.7 μm. Figure 4a shows a critical peak, but the magnitudes of both the critical peak and the drop in R are very small, of the order of 0.1% of the normal-state resistance. Interestingly, after the initial drop at 4 K, the resistance shows an upturn of 0.03 Ω below 2.4 K and 1.8 K. A similar upturn was reported in Co–Al junctions but the origin of this effect is unclear[7,8]. Such an upturn in R may also be present but not seen in all other samples in this study because it could be swamped by the large drop in R resulting from the much more substantial proximity effect. Subsequent to the measurement with the configuration shown in the inset of Fig. 4a, external leads to the electrodes were disconnected and the sample was returned to the FIB chamber and an extra W strip between the two voltage electrodes was added (see Fig. 4b, inset) and the sample was re-measured with the same current and voltage electrodes as that in Fig. 4a. The new W strip is not connected electrically. Interestingly, the critical peak and the superconducting drop were found to increase by two orders of magnitude, comparable to that shown in Fig. 2. This experiment shows that the critical peak requires only a superconducting electrode to be in contact with the nanowire; it is not necessary for the superconducting electrodes to be either a current or a voltage electrode. The result shown in Fig. 4b confirms that the proximity effect in the ferromagnetic Co nanowire is long ranged with a spatial extent that is of the order of several hundred nanometres.

We have also fabricated ferromagnetic Ni nanowires with a diameter of 60 nm using the electrodeposition method. Track-etched porous polycarbonate was used instead of AAO membrane[3], again with a variation in the wire diameter of around ±5 nm. Resistance measurements with superconducting W electrodes were made on such a Ni wire of 3 μm in length. Figure 5 shows R versus T under different magnetic fields and R versus H at different temperatures. In contrast to Co nanowires, both single-crystalline and polycrystalline nanowires were obtained in the electrodeposition process (see Supplementary Fig. S6) and we do

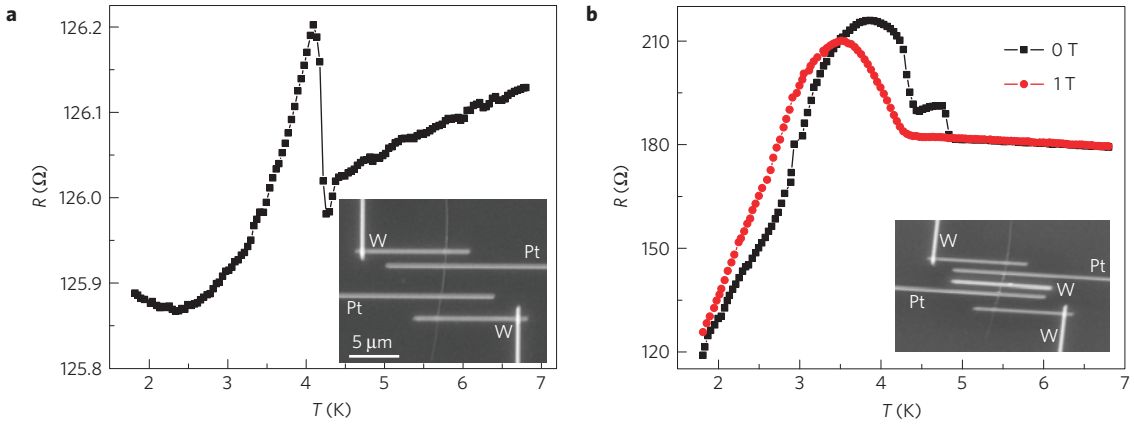

Figure 4 | Measurements using a combination of superconducting and non-superconducting electrodes. a, Resistance versus temperature of a 40 nm Co nanowire with two superconducting W current electrodes and two normal Pt voltage electrodes. The inset is a scanning electron micrograph of the measurement structure. ρ at 6 K is 5.3 μΩ cm. **b**, The critical resistance peak and superconducting drop are greatly enhanced by an extra W strip near the centre of the 40 nm Co nanowire. ρ at 6 K is increased to 7.6 μΩ cm.

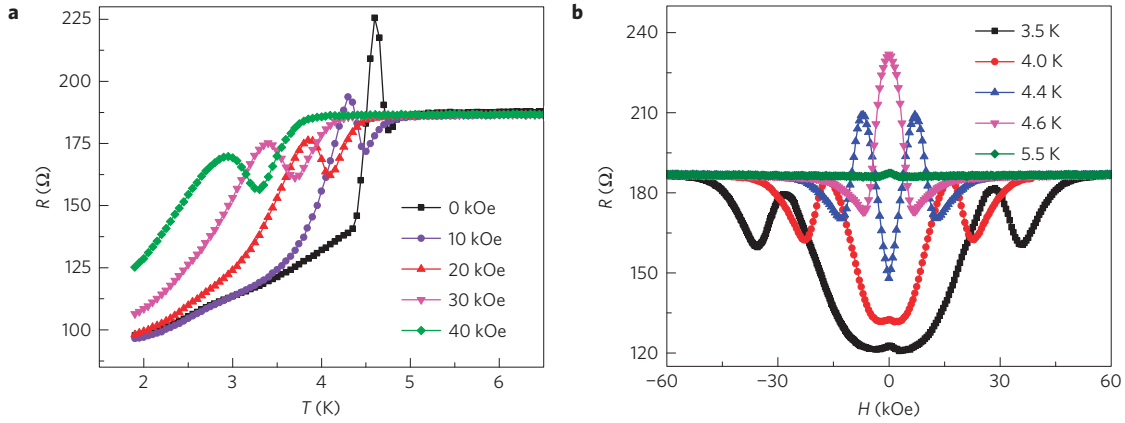

Figure 5 | Transport behaviour of a 60 nm Ni nanowire. a, Resistance as a function of temperature at different perpendicular magnetic fields for an individual 60 nm Ni nanowire with $L = 3$ μm. ρ at 6 K is 15.3 μΩ cm. **b**, Resistance versus magnetic field of a 60 nm Ni nanowire, with $L = 3$ μm, measured at temperatures of 3.5, 4.0, 4.4, 4.6 and 5.5 K. Small AMR peaks are seen at 3.5, 4.0 as well as 5.5 K.

not know if the wire measured is single crystal or polycrystalline. A critical peak and an incomplete superconducting drop, similar to that shown in Fig. 2, were observed. The low-temperature residual resistance (97.8 Ω at 1.9 K) is 52% of the normal-state resistance (187.7 Ω at 6 K). This suggests that the spatial extent of the proximity effect is again several hundred nanometres, similar to that of the Co wire. Similar to the 40 nm Co wire, the large (20% of the normal-state value) resistance peak near 4.6 K is preceded by a small dip. Interestingly, in the Ni nanowire we observe signatures of ferromagnetism (AMR) near zero field at 3.5 K and 4.0 K, indicating that at least a portion of the Ni wire, which has shown an 'incomplete' superconducting drop, is still ferromagnetic.

The expected singlet coherence length in Co nanowires is given by $\xi_F \approx \sqrt{\hbar D/k_B T_{Curie}}$ (ref. 12), where T_{Curie} is the Curie temperature and $D = (1/3)v_F l$ is the electron diffusion constant (here, v_F is the Co Fermi velocity $\sim 10^8$ cm s^{-1} and l is the mean free path). The experimentally measured resistivities yield Drude model estimates for the mean free paths of 1.8, 5.9, 6.5, 11, 7.7 and 3.9 nm for the samples shown respectively in Figs 1, 2a,b, 4a,b and 5 at 6 K. These numbers yield ξ_F respectively of 1.8, 3.3, 3.4, 4.5, 3.7 and 2.7 nm, which are much smaller than our observation of several hundred nanometres. The long-range proximity effect in mesoscopic ferromagnets may suggest the formation of spin-triplet-induced superconductivity[7,12,13]. It has been noted in the theoretical literature[7,13] that conversion from singlet to triplet superconductivity requires inhomogeneous magnetic moments. Although the Co nanowires must be single domain because we first saturate the magnetization and then do the zero field measurements, the attachment of the W electrodes by the FIB deposition process involves the bombardment of high-energy ions and heating of the nanowire. This process may very likely produce defects and inhomogeneous magnetic moments in W–Co contact regions. This is an interesting question worthy of systematic investigations.

The resistance peaks observed in our systems are distinct from resistance peaks reported previously in the literature. A resistance peak near the onset of the superconductivity was reported in lithographically fabricated systems of mesoscopic Al wires and strips connected to Al electrodes[24–26]. The peak was attributed to a non-equilibrium charge imbalance resulting from the different spatial gradients of the respective electrochemical potentials of the quasi-particles and the Cooper pairs at the normal-metal/superconductor interface[24,25]. The observed peak was found to be very sensitive to the applied magnetic field, suppressed by a tiny field of approximately 10 Oe, far smaller than the critical field of the superconductivity[24,26], and the resistive anomaly depended on the cooling history, disappearing on thermal cycling[26]. Furthermore, the 'charge imbalance' resistance peak behaviour was not observed in many other experiments on superconducting nanowires[21,27,28], superconducting bridges[29,30], and in proximity-induced superconductivity in narrow normal-metal (Cu or Ag)

wires with submicrometre superconducting electrodes (Al; ref. 31). In sharp contrast, the resistance peak observed in our Co and Ni nanowires is robust with respect to thermal cycling and persists even in the presence of a large (several T) magnetic field, indicating that it is distinct from the peak effect reported in refs 24–26.

Spin accumulation[32,33] has been suggested as the origin for the resistance peak observed in mesoscopic Fe–In junctions[5]. In that case, however, the absolute peak value (ΔR) was small ($\sim 10^{-8}\,\Omega$), as was the relative change from the normal-state resistance ($\Delta R/R \sim 0.05\%$). This spin-accumulation mechanism has been attributed to a contact resistance that arises from a mismatch between the spin-polarized current in the ferromagnet and the unpolarized current in the singlet superconductor[32,33]. Taking a simple model where the conductivity of spin-up electrons, $\sigma_\uparrow$, is larger than the conductivity $\sigma_\downarrow$ of spin-down electrons in the ferromagnet, one can define a measure of the 'transport polarization' $p = (\sigma_\uparrow - \sigma_\downarrow)/(\sigma_\uparrow + \sigma_\downarrow)$ and the total conductivity $\sigma_T = \sigma_\uparrow + \sigma_\downarrow$. Theoretical models show[32,33] that the resistance of a ferromagnet/normal-metal junction increases once the normal metal turns into a singlet superconductor. The increment in resistance is given by

$$\Delta R = \frac{p^2}{1-p^2}\left(\frac{l_{sd}}{\sigma_T A}\right)$$

where l_{sd} is the spin diffusion length in the ferromagnet and A is the area of the ferromagnet/normal-metal junction. For a ferromagnetic nanowire, the quantity in the parenthesis is equivalent to the resistance of a segment of the nanowire with length l_{sd}. On the basis of the bulk spin polarization of Co ($p \sim 0.42$; ref. 34) and an estimated value of $l_{sd} \sim 60$ nm in Co nanowires[35], the spin-accumulation mechanism predicts a substantially smaller resistance peak in the 1.5 μm nanowire ($\Delta R/R \sim 4\%$) than that observed in our experiments ($25\% < \Delta R/R < 100\%$). Furthermore, the spin-accumulation model assumes that the induced superconductivity is singlet, which seems inconsistent with the long-ranged nature of the proximity effect. This leads us to surmise that the spin-accumulation mechanism, at least as presented in refs 32,33, cannot simultaneously account for both the large resistance peak and the long-range proximity effect.

It would be desirable to carry out density of states measurements for the induced superconductivity in ferromagnetic nanowires[36] to see how it evolves as a function of the distance. Comparisons of such measurements with the Usadel theory[36,37] will provide useful information towards a quantitative theory of transport through proximity-induced superconductivity in a ferromagnetic nanowire, and may allow confirmation of the triplet nature of the superconductivity. However, our current experimental set-up is not amenable to density of states measurement, because our contacts are not tunnel junctions.

Our systematic study of ferromagnetic Co and Ni nanowires connected to superconducting W electrodes has demonstrated the spatial extent of the proximity effect to be of the order of 500 nm, similar to that found in paramagnetic gold nanowires. For Co and Ni wires that do not achieve zero resistance at low temperatures, the resistance shows an unexpected peak immediately before the onset of superconductivity, which cannot be easily explained on the basis of the existing theoretical models. This peak was not seen in non-magnetic Au nanowires. Our study underscores the need for a direct probe of the pairing symmetry and magnetic behaviour in the nanowire, to demonstrate the coexistence of superconductivity and ferromagnetism. To test the universality of the phenomena reported here, it will be interesting to ascertain if the observed phenomena can be replicated with standard superconducting electrodes other than FIB-deposited W strips, including conventional as well as high-T_C superconductors, and also in ferromagnetic thin films[38].

Methods

The electrolyte for Co nanowires is made by mixing 200 g l^{-1} $CoSO_4$ and 40 g l^{-1} H_3BO_3, with pH = 1.0 adjusted by 1 M H_2SO_4. Before electrodeposition, a 200-nm-thick Ag film is deposited on the backside of an AAO membrane, which acts as the working cathode. The nanowires are deposited at a potential of $V = -1.45$ V with reference to a Ag/AgCl electrode, using Pt as the counter-electrode. After electrodeposition, nanowires are released from the host membrane by dissolving it in 1 M NaOH solution. Three batches of Co nanowires were fabricated with this method and ~5–10 nanowires from each batch were studied with TEM. All wires studied were found to be single crystal.

The electrolyte for Ni nanowire preparation contains a mixture of 100 g l^{-1} $NiSO_4 \cdot 6H_2O$, 30 g l^{-1} $NiCl_2 \cdot 6H_2O$ and 40 g l^{-1} H_3BO_3 solution. The pH value was adjusted to 2 with 1 M H_2SO_4 solution. Ni nanowire arrays were fabricated by electrodeposition into the pores of a polycarbonate membrane. One side of the membrane was coated with a 200-nm-thick layer of thermally evaporated Ag, which acted as the cathode. Pt was used as the anode and the electrodeposition was carried out at a constant voltage of −1.00 V with respect to a Ag/AgCl reference electrode. As noted in the text, both polycrystalline and single-crystal-line Ni nanowires are found in the same porous membrane with this growth method.

Received 12 October 2009; accepted 8 February 2010; published online 21 March 2010

References

1. De Gennes, P. G. Boundary effects in superconductors. *Rev. Mod. Phys.* **36,** 225–237 (1964).
2. van Dover, R. B., de Lozanne, A. & Beasley, M. R. Superconductor–normal–superconductor microbridges: Fabrication, electrical behaviour, and modelling. *J. Appl. Phys.* **52,** 7327–7343 (1981).
3. Wang, J. *et al.* Proximity-induced superconductivity in nanowires: Minigap state and differential magnetoresistance oscillations. *Phys. Rev. Lett.* **102,** 247003 (2009).
4. Buzdin, A. I. Proximity effects in superconductor–ferromagnet heterostructures. *Rev. Mod. Phys.* **77,** 935–976 (2005).
5. Chiang, Yu. N., Shevchenko, O. G. & Kolenov, R. N. Manifestation of coherent and spin-dependent effects in the conductance of ferromagnets adjoining a superconductor. *Low Temp. Phys.* **33,** 314–320 (2007).
6. Aumentado, J. & Chandrasekhar, V. Mesoscopic ferromagnet–superconductor junctions and the proximity effect. *Phys. Rev. B* **64,** 054505 (2001).
7. Bergeret, F. S., Volkov, A. F. & Efetov, K. B. Odd triplet superconductivity and related phenomena in superconductor–ferromagnet structures. *Rev. Mod. Phys.* **77,** 1321–1373 (2005).
8. Giroud, M., Courtois, H., Hasselbach, K., Mailly, D. & Pannetier, B. Superconducting proximity effect in a mesoscopic ferromagnetic wire. *Phys. Rev. B* **58,** R11872–R11875 (1998).
9. Petrashov, V. T., Sosnin, I. A., Cox, I., Parsons, A. & Troadec, C. Giant mutual proximity effects in ferromagnetic/superconducting nanostructures. *Phys. Rev. Lett.* **83,** 3281–3284 (1999).
10. Pena, V. *et al.* Coupling of superconductors through a half-metallic ferromagnet: Evidence for a long-range proximity effect. *Phys. Rev. B* **69,** 224502 (2004).
11. Sosnin, I., Cho, H., Petrashov, V. T. & Volkov, A. F. Superconducting phase coherent electron transport in proximity conical ferromagnets. *Phys. Rev. Lett.* **96,** 157002 (2006).
12. Keizer, R. S. *et al.* A spin triplet supercurrent through the half-metallic ferromagnet CrO_2. *Nature* **439,** 825–827 (2006).
13. Bergeret, F. S., Volkov, A. F. & Efetov, K. B. Long-range proximity effects in superconductor–ferromagnet structures. *Phys. Rev. Lett.* **86,** 4096–4099 (2001).
14. Tian, M. L. *et al.* Penetrating the oxide barrier *in situ* and separating freestanding porous anodic alumina films in one step. *Nano Lett.* **5,** 697–703 (2005).
15. Hernandez-Ramirez, F. *et al.* Electrical properties of individual tin oxide nanowires contacted to platinum electrodes. *Phys. Rev. B* **76,** 085429 (2007).
16. Kumar, N. *et al.* Investigation of superconductivity in electrochemically fabricated AuSn nanowires. *Nanotechnology* **19,** 365704 (2008).
17. Tian, M. L. *et al.* Superconductivity and quantum oscillations in crystalline Bi nanowire. *Nano Lett.* **9,** 3196–3202 (2009).
18. Sadki, E. S., Ooi, S. & Hirata, K. Focused-ion-beam-induced deposition of superconducting nanowires. *Appl. Phys. Lett.* **85,** 6206–6208 (2004).
19. Li, W., Fenton, J. C., Wang, Y., McComb, D. M. & Warburton, P. A. Tunability of the superconductivity of tungsten films grown by focused-ion-beam direct writing. *J. Appl. Phys.* **104,** 093913 (2008).
20. Schmidt, V. V. in *The Physics of Superconductors: Introduction to Fundamentals and Applications* (eds Muller, P. & Ustinov, A. V.) (Springer, 1997).
21. Tian, M. L. *et al.* Dissipation in quasi-one-dimensional superconducting single-crystal Sn nanowires. *Phys. Rev. B* **71,** 104521 (2005).
22. Vila, L. *et al.* Transport and magnetic properties of isolated cobalt nanowires. *IEEE Trans. Magn.* **38,** 2577–2579 (2002).

23. Brands, M. & Dumpich, G. Experimental determination of anisotropy and demagnetizing factors of single Co nanowires by magnetoresistance measurements. *J. Appl. Phys.* **98,** 014309 (2005).
24. Santhanam, P., Shi, C. C., Wind, S. J., Brady, M. J. & Bucchignano, J. J. Resistance anomaly near the superconducting transition temperature in short aluminium wires. *Phys. Rev. Lett.* **66,** 2254–2257 (1991).
25. Park, M., Isaacson, M. S. & Parpia, J. M. Resistance anomaly and excess voltage in inhomogeneous superconducting aluminium thin films. *Phys. Rev. B* **55,** 9067–9076 (1997).
26. Arutyunov, K. Yu., Presnov, D. A., Lotkhov, S. V., Pavolotski, A. B. & Rinderer, L. Resistive-state anomaly in superconducting nanostructures. *Phys. Rev. B* **59,** 6487–6498 (1999).
27. Tian, M. L. *et al.* Suppression of superconductivity in zinc nanowires by bulk superconductors. *Phys. Rev. Lett.* **95,** 076802 (2005).
28. Zgirski, M., Riikonen, K., Touboltsev, V. & Arutyunov, K. Size dependent breakdown of superconductivity in ultranarrow nanowires. *Nano Lett.* **5,** 1029–1033 (2005).
29. Wang, J. *et al.* Anomalous magnetoresistance oscillations and enhanced superconductivity in single-crystal Pb nanobelts. *Appl. Phys. Lett.* **92,** 233119 (2008).
30. Bezryadin, A., Lau, C. N. & Tinkham, M. Quantum suppression of superconductivity in ultrathin nanowires. *Nature* **404,** 971–974 (2000).
31. Ciurtois, H., Gandit, Ph. & Pannetier, B. Proximity-induced superconductivity in a narrow metallic wire. *Phys. Rev. B* **52,** 1162–1166 (1995).
32. Jedema, F. J., van Wees, B. J., Hoving, B. H., Filip, A. T. & Klapwijk, T. M. Spin-accumulation-induced resistance in mesoscopic ferromagnet–superconductor junctions. *Phys. Rev. B* **60,** 16549–16552 (1999).
33. Fal'ko, V. I., Volkov, A. F. & Lambert, C. Interplay between spin-relaxation and Andreev reflection in ferromagnetic wires with superconducting contacts. *Phys. Rev. B* **60,** 15394–15397 (1999).
34. Soulen, R. J. Jr *et al.* Measuring the spin polarization of a metal with a superconducting point contact. *Science* **282,** 85–88 (1998).
35. Piraux, L., Dubois, S., Fert, A. & Belliard, L. The temperature dependence of the perpendicular giant magnetoresistance in Co/Cu multilayered nanowires. *Eur. Phys. J. B* **4,** 413–420 (1998).
36. Gueron, S., Pothier, H., Birge, N. O., Esteve, D. & Devoret, M. H. Superconducting proximity effect probed on a mesoscopic length scale. *Phys. Rev. Lett.* **77,** 3025–3028 (1996).
37. Usadel, K. D. Generalized diffusion equation for superconducting alloys. *Phys. Rev. Lett.* **25,** 507–509 (1970).
38. Ozatay, O. *et al.* Sidewall oxide effects on spin-torque- and magnetic-field-induced reversal characteristics of thin-film nanomagnets. *Nature Mater.* **7,** 567–573 (2008).

Acknowledgements

This work was supported by the Penn State MRSEC under NSF grant DMR-0820404 and the Pennsylvania State University Materials Research Institute Nano Fabrication Network and the National Science Foundation Cooperative Agreement No. 0335765, National Nanotechnology Infrastructure Network, with Cornell University. We are grateful to P. A. Lee for helpful discussions. We thank J. Cardellino and D. Rench for magnetic force microscopy measurements.

Author contributions

J.W., M.H.W.C. and M.T. planned the experiments. J.W., M.S., N.K. and B.L. carried out the experiments. J.W., M.H.W.C., C.S., J.K.J., N.S., M.T. and T.E.M. analysed the data.

Additional information

The authors declare no competing financial interests. Supplementary information accompanies this paper on www.nature.com/naturephysics. Reprints and permissions information is available online at http://npg.nature.com/reprintsandpermissions. Correspondence and requests for materials should be addressed to J.W. or M.H.W.C.